Pure & Appl. Chem., Vol. 65, No. 8, pp. 1825–1847, 1993.
Printed in Great Britain.
© 1993 IUPAC

INTERNATIONAL UNION OF PURE
AND APPLIED CHEMISTRY

MACROMOLECULAR DIVISION
COMMISSION ON POLYMER CHARACTERIZATION AND PROPERTIES
WORKING PARTY ON STRUCTURE AND PROPERTIES
OF COMMERCIAL POLYMERS*

MOLECULAR CHARACTERISTICS AND CRYSTALLINE STRUCTURE OF ETHYLENE-DIMETHYLAMINOETHYL-METHACRYLATE COPOLYMERS

(Technical Report)

Prepared for publication by

T. OHMAE[1], S. HOSODA[1], H. TANAKA[1], H. KIHARA[1], B. JIANG[2], Q. YING[3], R. QIAN[3], T. MASUDA[4] AND A. NAKAJIMA[4]

[1]Chiba Research Laboratory, Sumitomo Chemical Co. Ltd., Chiba 299-02, Japan
[2]Changchun Institute of Applied Chemistry, Chinese Academy of Sciences, Changchun, Jilin, China
[3]Institute of Chemistry, Chinese Academy of Sciences, Beijing, China
[4]Research Center for Biochemical Engineering, Kyoto University, Kyoto 606, Japan

for the East Asia Sub-Group

Chairman: A. Nakajima; *Secretary*: T. Masuda; *Members*: J. H. Byon; C. R. Choe; H. He; M. Hirami; M. Isshi; B. Jiang; J. C. Jung; S. Kataoka; C. K. Kim; C. Y. Kim; K. U. Kim; S. C. Kim; Y. Kometani; Y. Kubouchi; J. Li; N. Nagata; K. Nakayama; T. Ohmae; T. Okamoto; R. Qian; K. Sakamoto; S. Shimotsuma; S. Suzuki; S. Tsuchiya; L. Wu; J. K. Yeo; A. Yoshioka.

*Membership of the Working Party during the preparation of this report (1986–92) was as follows:

Chairman: 1987–89 H. H. Meyer (FRG); 1989–91 D. R. Moore (UK); *Secretary*: 1987–89 D. R. Moore (UK); 1989–91 M. Laún (FRG); *Members*: G. Ajroldi (Italy); M. Bargain† (France); M. Bevis† (UK); C. B. Bucknall (UK); M. Cakmak† (USA); J. M. Cann (UK); M. J. Cawood† (UK); A. Cervenka (Netherlands); D. Constantin (France); Van Dijk‡ (Netherlands); M. J. Doyle (USA); M. Fleissner (FRG); Franck‡ (FRG); H. G. Fritz (FRG); P. H. Geil (USA); A. Ghijsels (Netherlands); S. K. Goyal† (Canada); D. J. Groves (UK); P. S. Hope (UK); T. A. Huang† (USA); R. J. Koopmans‡ (Netherlands); V. Leo (Belgium); J. Lyngaae-Jorgensen† (Denmark); F. H. J. Maurer† (Netherlands); J. Meissner (Switzerland); H. Motz† (FRG); A. Plochocki (USA); W. Retting (FRG); G. Schorsch‡ (France); H. Schwickert‡ (FRG); H. Schuch† (FRG); J. C. Seferis (USA); S. S. Sternstein (USA); L. A. Utracki (Canada); G. Vassilatos (USA); T. Vu-Khanh† (Canada); J. L. White (USA); C. Wrotecki† (France); H. H. Winter (USA); H. G. Zachman (FRG).

†1989–91 ‡1987–89

Republication of this report is permitted without the need for formal IUPAC permission on condition that an acknowledgement, with full reference together with IUPAC copyright symbol (© 1993 IUPAC), is printed. Publication of a translation into another language is subject to the additional condition of prior approval from the relevant IUPAC National Adhering Organization.

Molecular characteristics and crystalline structure of ethylene-dimethylaminoethylmethacrylate copolymers (Technical Report)

ABSTRACT: The relationship between molecular and crystalline structural characteristics of the ethylene -dimethylaminoethylmethacrylate copolymers (EDAM) was investigated and related to melt flow index MI and average gross content of DAM comonomer, in comparison with low density polyethylene (LDPE) produced by the common high-pressure radical polymerization process. Although the average molecular weight and its distribution are influenced predominantly by the polymerization conditions, DAM-content seems not to depend significantly on molecular weight according to the GPC-FT/IR measurement.
Comonomer sequence distributions were determined quantitatively with the ^{13}C-NMR spectra entirely assigned by DEPT and ^{1}H-^{13}C COSY techniques. The result suggests the alternating copolymerization tendency and suprisingly coincides with the simulation out-puts based on the assumption of continuous complete mixing reactor model, using Mayo-Lewis equation and the same Q-e values as previously reported on different types of copolymers such as EVA and St·DAM (VA;vinylacetate, St;styrene).
It was confirmed by WAXD and SAXS analyses that the crystallinity X_c and the thickness of lamellar crystal ℓ_c decreased with increasing DAM-content, whereas the a-lattice and b-lattice dimensions enlarged. X_c and ℓ_c can definitely be correlated to the heats of fusion and crystallization measured by DSC. The average size of spherulites measured with light scattering photometry tends to be enlarged with decreasing molecular weight (increasing MI) and DAM-content.

INTRODUCTION

Copolymers (EDAM) of ethylene with N, N-dimethylaminoethylmethacrylate (DAM) are manufactured by the high-pressure radical polymerization process common to low density polyethylenes (LDPE). The copolymers are useful and important particularly as dyeing modifiers for polypropylene fibers (ref. 1-5). The dimethylamino-group branches afford effective dyesites toward acid- or premetallized-type dyestuffs, while the polyethylenic main chain contributes to fine dispersing into polypropylene, and thus the smooth melt-spinning of the blended compound is attained.

The melt flow index MI, an industrial standard of melt fluidity parameter which fairly reflects the average molecular weight, and the average gross content of DAM monomer are the macroscopic copolymer characteristics controllable during the polymerization operation.

Therefore, the practical properties in actual applications have so far been evaluated merely in connection with these two characteristics.

The East Asia Sub-Group meeting of IUPAC Working Party Ⅳ-2-1 has been working to investigate the molecular microstructures of the EDAM copolymer chain and the higher order structural characteristics, such as crystalline/amorphous size, spherulite size and thermal properties, in relation to the above macroscopic copolymer characters. Some kinds of LDPE produced under nearly the same polymerization conditions were also studied for comparative considerations.

This paper is concerned with the results on experiments and discussion which have been made by the Sub-Group in the last four years. Particular emphasis will be placed to highlight the copolymerization mode between ethylene and DAM monomer, making reference to a simulation based on the Q-e values of each comonomer, and also the correlation of crystalline and thermal characteristics.

EXPERIMENTAL

Materials

Samples of EDAM copolymers and low density polyethylenes (LDPE) provided by Sumitomo Chemical are listed in Table 1. All the samples were produced by continuous radical polymerization processes with a vigorously stirred vessel-type reactor under the conditions of 1300 ~2300kg/㎠ and 165~210℃.

DA1701 is the only commercial product, and the others are all non-commercial samples.

Measurements

DAM-contents of EDAM copolymer samples were calculated from the results of N-content analysis by Kjeldahl method.

Melt flow index MI was measured at 190℃ with 2.16kg load according to ASTM D1238.

Intrinsic viscosity $[\eta]$ was measured in tetralin solution at 135℃ by using Ubbelohde's viscometer.
Density was measured according to ASTM D1505 at 20℃ after annealing.

Thermogravimetric analyses (TGA) were carried out to investigate thermochemical reaction under N_2 atmosphere during temperature elevation from 20℃ to 600℃ at the rate of 10℃/min, using a SEIKO ELECTRICS model TGA/DTA 200 analyzer.

Exothermic and endothermic curves were measured using a SEIKO ELECTRICS model DSC 200 (Differential Scanning Calorimeter). Each sample of about 5 mg was held at 150 ℃ for 5 min, cooled and heated at the rate of 10℃/min. Heat of fusion $\triangle H_f$ was calculated from the area of the endothermic curve using indium sample (28.5 joul/g) as a standard, and the peak point of the curve was taken as the melting temperature T_m. Heat of crystallization $\triangle H_c$ and crystallization temperature T_c were also determined similarly with the exothermic curve.

Average molecular weights, M_n and M_w, and molecular weight distribution (MWD) were measured from calibration curve obtained on polystyrene by gel permeation chromatography (GPC), TOSOH HLC 811, equipped with both a refractometer and a Chromatix low-angle laser

TABLE 1. Molecular characteristics and thermal properties of EDAM copolymers and low density polyethylenes (LDPE).

EDAM	Content			M I	$[\eta]$	Density	Thermal properties			
	N	D A M			Tetralin,	at 20°C	T_m	T_c	ΔH_f	ΔH_c
	wt%	wt%	mol%	g/10min.	135°C	g/cm³	°C	°C	joul/g	joul/g
DA 3032	3.5	39	10.2	300	0.49	0.9392	65.5	48.1	21.8	− 15.9
DA 3002	2.7	30	7.1	400	0.49	0.9345	83.6	61.6	42.3	− 38.5
DA 1701	2.5	28	6.5	100	0.59	0.9358	88.0	68.0	45.2	− 46.5
DA 3012	2.5	28	6.5	20	0.77	0.9351	87.8	64.5	43.9	− 44.4
DA 3023	1.8	20	4.3	400	0.51	0.9291	92.3	73.2	62.8	− 61.5
DA 3011	1.8	20	4.3	90	0.59	0.9313	93.0	72.7	56.5	− 58.6
DA 3013	1.8	20	4.3	17	0.66	0.9317	96.3	77.0	68.2	− 62.4
DA 3014	1.8	20	4.3	2	0.95	0.9303	99.3	81.7	74.5	− 69.9
DA 3024	1.3	15	3.0	400	0.51	0.9274	93.9	75.5	66.5	− 77.4
DA 3005	1.3	15	3.0	6	0.79	0.9317	97.8	80.1	72.8	− 68.2
PE 3341	−	−	−	2	0.94	0.9341	120.6	107.7	152	−162
PE 3246	−	−	−	2	0.99	0.9276	113.8	99.8	126	−146

light scattering apparatus. Tetrahydrofuran solutions containing 0.15 wt% copolymer and 0.5 wt% n-butylamine were fed into a column controlled at 60°C.

The absolute weight-average molecular weight of the sample DA1701 was measured by low-angle laser light scattering method in the Institute of Chemistry, Chinese Academy of Sciences, in three solvents, o-dichlorobenzene, chlorobenzene and cyclohexane. The refractive index increments of the copolymer solutions in these solvents at 50°C were determined on an OHTSUKA model RM 102 differential refractometer, using an incandescent light source with a λ =6328 Å interference filter. The determination of the apparent molecular weight M_{app} in the three solvents was made on a Chromatix model KMX-6 low-angle laser light scattering photometer using a He-Ne laser of λ =6328 Å as the light source. The detailed procedure to evaluate M_w will be described later.

The molecular weight dependence of copolymer composition was measured using GPC, TOSOH HLC 802UR, equipped with a FT-IR spectrometer (Perkin Elmer 1750). Chloroform containing a small amount of n-butylamine (0.2 wt%) was used as an eluent. The system was maintained at 40°C. IR spectrum acquisitions were carried out continuously during the elution. DAM-content was evaluated from the peak intesity ratio of the band at 1720 cm^{-1}, $\nu_{C=O}$, to that at 2929 cm^{-1}, $\nu_{as}(CH_2)$. The intensity ratios for about 30 spectra obtained in every 30 sec were averaged to make one data point.

^{13}C-NMR spectra were obtained on a Bruker AM 400 spectometer operating at 100.6 MHz at 60°C. Polymer solutions for NMR measurement were prepared in deutero-chloroform with concentration maintained at 10 % by weight. Tetramethylsilane was used as a chemical shift reference. The conditions for measurement were as follows: pulse interval, 10 sec; spectral width, 29 KHz; pulse width, 4.8 μsec (90°); acquisition time, 0.6 sec; number of data points per spectrum, 32 K.

DEPT (Distortionless Enhancement by Polarization Transfer) spectrum and ^{13}C-^{1}H COSY (Correlation 2D spectoscopy) were measured in order

to assign NMR peaks more precisely.

X-ray crystallinity X_c and the thickness of lamellar crystal ℓ_c were determined using wide angle X-ray diffraction (WAXD) and small angle X-ray scattering (SAXS), respectively. WAXD and SAXS were measured with a Rigaku RAD-RB X-ray diffractometer. Lamellar thickness ℓ_c was calculated from the following relationship, considering a two-phase model for EDAM solid;

$$\ell_c = 0.85X_c \cdot L/(1 - 0.15X_c) \quad (1)$$

where L is a long period determined by SAXS, and the densities of crystalline and amorphous phases were taken to be 1.00 and 0.86, respectively (ref. 6).

Lamellar crystalline morphology of EDAM was observed by transmission electron microscopy (TEM). A hot-press molded sample specimen was sectioned at room temperature with an ultramicrotome and stained by phosphotungstenic acid (PTA) aqueous solution at 60℃ for 1 hour. It is supposed that only amorphous phase is dyed as a result of a relatively easier penetration of the staining reagents, so a clear contrast is visible only when the lamellae and the amorphous phase are perpendicular to the surface of the thin section, and under this condition, the lamellar thickness can be directly measured. The thickness was measured with about 200 lamellae and the number average thickness was calculated.

Morphological study on spherulites was carried out in the Changchun Institute of Applied Chemistry, Chinese Academy of Sciences, with Light Scattering System JSY-390, made by the workshop of the Institute. Samples for the measurement were hot-press molded at 140℃ and quenched in air. The radius of spherulite R_s was evaluated with Stein's procedure (ref. 7) shown below:

$$4.1 = (4\pi/\lambda)\, R_s \cdot \sin(\theta_{max}/2) \quad (2)$$

where $\lambda = 6328$ Å is the wavelength of light obtained from a He-Ne laser, and θ_{max} is the scattering angle.

RESULTS AND DISCUSSION

Molecular characteristics

DAM-content, MI, $[\eta]$, and density of EDAM copolymers and LDPE used in this study are summarized in Table 1.

Logarithms of MI, a parameter of melt viscosity, decrease almost linearly with increasing solution viscosity $[\eta]$ as shown in Fig. 1, and there is little difference between the EDAM copolymers and EVA (ethylene-vinylacetate) copolymers prepared by the same high-pressure polymerization process, in spite of differences in polarity and bulkiness of side residures of each copolymer.

DAM-content dependence on density for EDAM copolymers is shown in Fig. 2, where a moderate similarity with EVA copolymers (broken line) is seen as a function of molar concentration of DAM and VA.

Thermal characteristics

Some representative DSC heating and cooling curves are shown in Figs. 3 and 4, respectively. T_m, T_c, ΔH_f and ΔH_c obtained from those curves are summarized in Table 1 together with those of

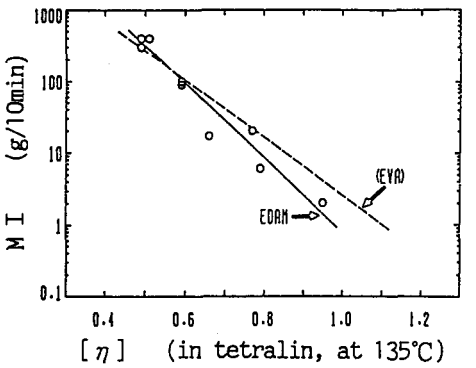

Fig. 1. MI vs. [η] correlation for EDAM copolymers (open circles, solid line) and EVA copolymers (broken line).

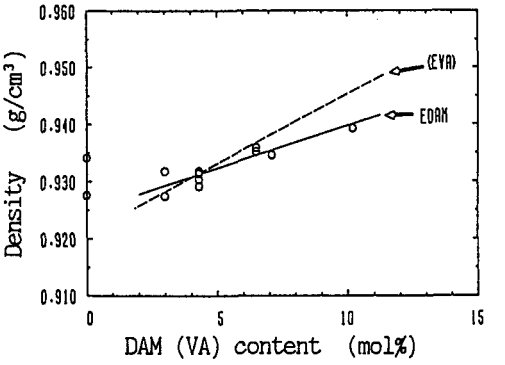

Fig. 2. Density vs. DAM-content correlation for EDAM copolymers (open circles) referred to EVA copolymers (broken line).

LDPE. Melting temperature T_m and crystallization temperature T_c decrease with increasing DAM-content as shown in Fig. 5, where fairly good agreement with EVA series (broken lines) are seen. It might be suggested that the degree of defective influence on crystalline structure by DAM-side chain is approximately close to that by VA-side chain. Both the heats of fusion $\triangle H_f$ and of crystallization $\triangle H_c$ are strongly dependent on DAM-content as shown in Figs. 6 and 7, respectively, which are consistent with the great decrease in lamellar thickness due to a little insertion of DAM units, as will be mentioned in the later section of this paper.

Figure 8 illustrates TGA curves of several EDAM copolymers of different DAM-contents and LDPE. It is apparent from the curves that thermal degradation of EDAM copolymer proceeds in two steps. The first region of the degradation could be defined approximately as from 250°C to 440°C, and the second one from 440°C to 500°C. An approximately linear relationship between weight loss in the first step degradation and DAM-content was held as shown in Fig. 9. The slope of the line found, 0.565, is just the molecular weight ratio of $(CH_3)_2NC_2H_4OH$ to DAM, which strongly suggests that the first thermal degradation occurred at the ester-bond position to eliminate dimethylaminoethanol.

Average molecular weight

Number- and weight-average molecular weight, M_n and M_w, based on the calibration with polystyrene, and the molecular weight distribution parameter M_w/M_n were measured by GPC and are listed in Table 2. Viscosity-average molecular weights M_v were also calculated as listed in the table, applying the Harris equation (ref. 8) for the samples of LDPE produced under nearly the same conditions as EDAM copolymers.

$$[\eta] = 1.35 \times 10^{-3} M_v^{0.63} \qquad (3)$$

where $[\eta]$ is the intrinsic viscosity. Molecular weight distribution (MWD) was recognized to be narrow for EDAM copolymerized under lower-temperature and/or higher-pressure condition like a normal tendency in LDPE, regardless of obscure correlation with DAM-content.

Regarding the copolymer DA1701, the determination of the absolute value of weight-average molecular weight M_w was carried out by low-

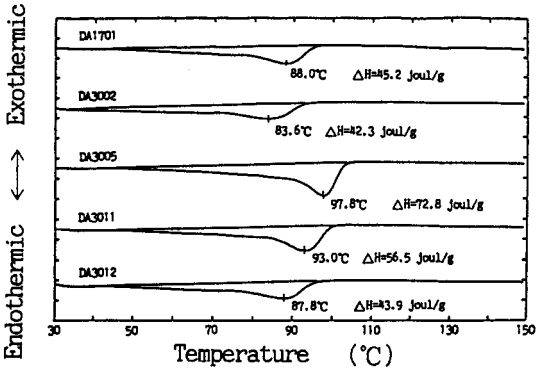

Fig. 3. DSC endothermic curves of EDAM copolymers.

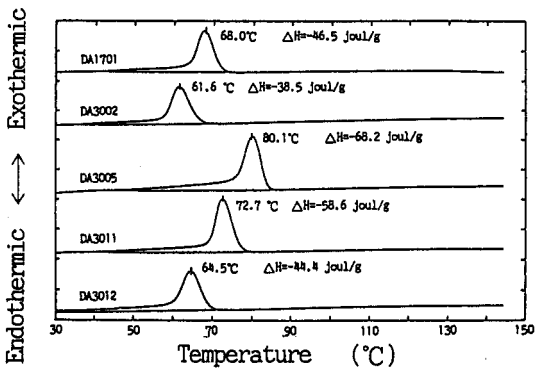

Fig. 4. DSC exothermic curves of EDAM copolymers.

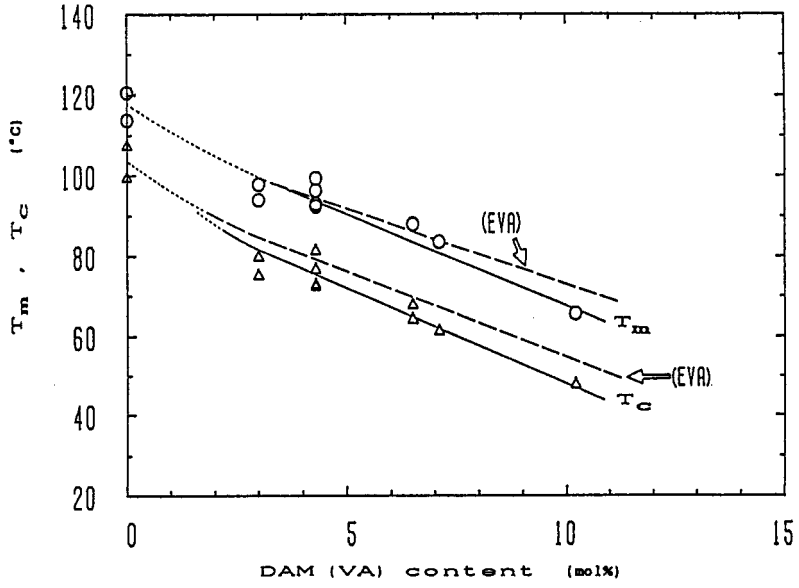

Fig. 5. T_m and T_c vs. DAM-content correlation for EDAM copolymers (circles and triangles) referred to EVA copolymers (broken lines).

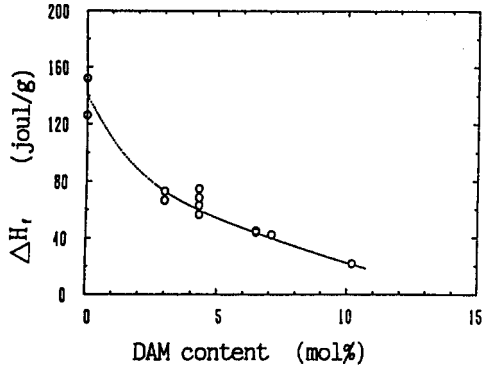

Fig. 6. Influence of DAM-content on heat of fusion, ΔH_f.

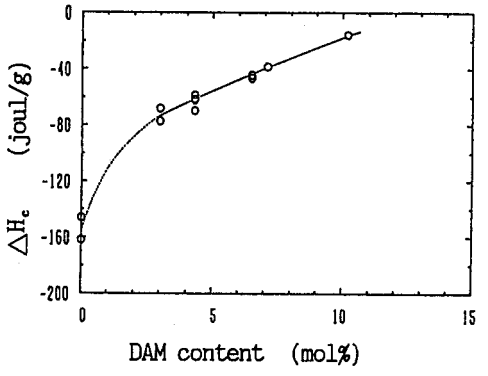

Fig. 7. Influence of DAM-content on heat of crystallization, ΔH_c.

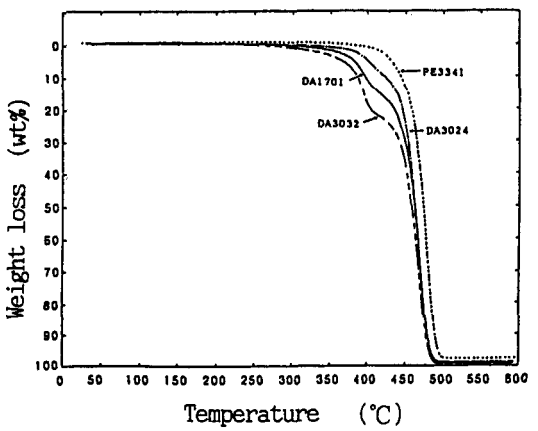

Fig. 8. Thermogravimetric analyses of EDAM copolymers and LDPE.

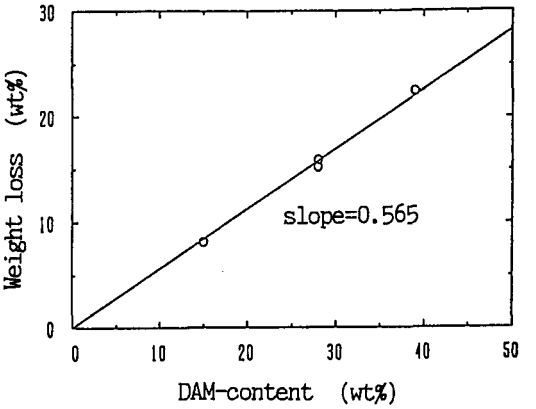

Fig. 9. Weight loss in the first step degradation vs. DAM-content correlation for EDAM copolymers.

angle laser light scattering (LALLS) experiments in three solvents of different refractive indices according to the theory of Benoît and Froelich (ref. 9).

$$M_{app} = M_w + 2P(f_E - f_D)/f + Q(f_E - f_D)^2/f^2 \qquad (4)$$

where M_{app} is the apparent molecular weight of EDAM as evaluated from the light scattering data in each solvent, f_E, f_D, and f are the refractive index increments of the solutions of homo-polyethylene, homo-poly(DAM) and EDAM copolymer, respectively, in each solvent, and P and Q are two parameters. The refractive index n_D of homo-poly(DAM) is calculated from the empirical relation

$$n_{EDAM} = W_E\, n_E + (1 - W_E)\, n_D \qquad (5)$$

where n_{EDAM} is the refractive index of EDAM copolymer and W_E (0.72) is the weight fraction of ethylene in the copolymer, which is found from N-analysis. The value of n_{EDAM} was estimated to be 1.479 based on GPC measurement in toluene at 50°C, whereas n_E was taken as that of LDPE to be 1.510 from the literature (ref. 10). Consequently, n_D is calculated to be 1.395.

The apparent molecular weight M_{app} can be evaluated from eqs. (6) and (7) by extrapolating the linear plot of $HC/\Delta R_\theta(C)$ vs. C to C=0,

$$HC/\Delta R_\theta(C) = 1/M_{app} + 2A_2C \qquad (6)$$

$$H = 2\pi^2/(\lambda^4 N)(1+\cos^2\theta)n^2 f^2 \qquad (7)$$

where $R_\theta(C)$ is the increment of the Rayleigh ratio of the solution at the scattering angle θ and concentration C, A_2 is the second Virial coefficient, λ is the wavelength of incident light, and N is the Avogadro number. The optical constants of the solution are listed in Table 3 and the light scattering data are presented in Fig. 10. The fitting of the data of M_{app} as a quadratic function of $(f_E - f_D)/f$ was accomplished by approximating the value of $(f_E - f_D)$ to the value of $(n_E - n_D)$, as shown in Fig. 11, from which M_w of DA1701 and the parameters P and Q are evaluated; $M_w = 4.52 \times 10^4$, $P = 2.32 \times 10^3$ and $Q = 8.68 \times 10^2$.

TABLE 2. Average molecular weight measured by GPC.

EDAM	DAM content wt%	M I g/10min.	M_n [a] $\times 10^{-4}$	M_w [a] $\times 10^{-4}$	M_w/M_n	$[\eta]$ [b] dl/g	M_v [c] $\times 10^{-4}$
DA 3032	39	300	3.37	7.63	2.3	0.49	1.16
DA 3002	30	400	1.50	3.20	2.1	0.49	1.16
DA 1701	28	100	2.84	6.09	2.1	0.59	1.55
DA 3023	20	400	2.43	8.88	3.7	0.51	1.23
DA 3011	20	90	2.64	11.2	4.2	0.59	1.55
DA 3013	20	17	2.94	8.29	2.8	0.66	1.86
DA 3014	20	2	7.80	25.4	3.3	0.95	3.31
PE 3341	-	2	- [d]	- [d]	-	0.94	3.25
PE 3246	-	2	- [d]	- [d]	-	0.99	3.53

a) reduced to polystyrene
Apparatus: TOSOH HLC 811
Conditions: THF solution containing n-butylamine (0.5%), 60℃
b) Intrinsic viscosity: tetralin solution, 135℃
c) calculated by Harris equation $[\eta]=1.35\times10^{-3}M_v^{0.63}$
d) Insoluble in THF solvent at 60℃

TABLE 3. Optical constants of the EDAM solution at 50℃ and M_{app} observed.

Solvent	n (λ =6328 Å)	f	$M_{app}\times10^{-4}$
o-dichlorobenzene	1.5383	-0.0727	4.06
chlorobenzene	1.5027	-0.0466	3.96
cyclohexane	1.4083	-0.0720	5.54

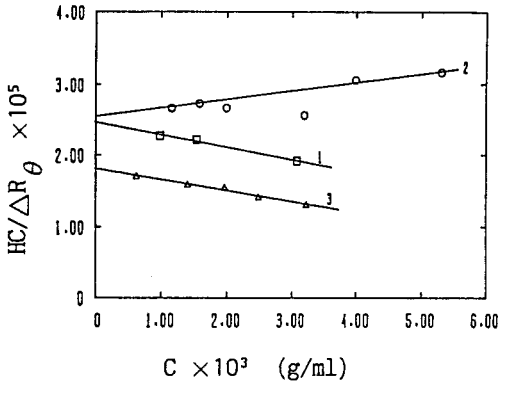

Fig. 10. Light scattering data of DA1701 in three solvents. (1:o-dichlorobenzene, 2:chlorobenzene, 3:cyclohexane)

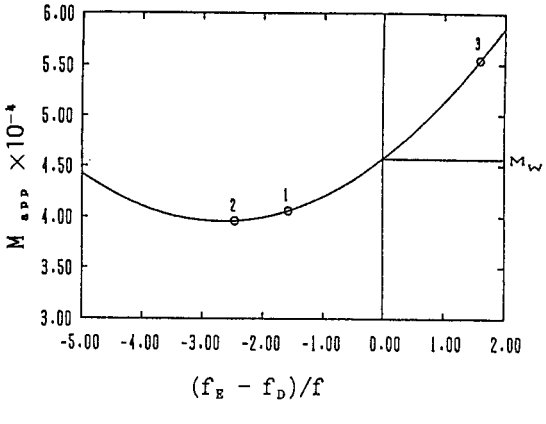

Fig. 11. Plot of M_{app} vs. $(f_E-f_D)/f$ for DA1701 in three solvents fitted to eq. 4. (1:o-dichlorobenzene, 2:chlorobenzene, 3:cyclohexane)

Molecular weight dependence of copolymer composition

Molecular weight dependence of DAM-content in EDAM copolymers evaluated by means of GPC-FT/IR system is shown in Fig. 12. The peak intensity ratio (I_{1720}/I_{2929}), which is a measure of DAM-content, does not show any particular dependence on molecular weight (chain length) in the region of the main part of MWD, though it slightly increases near the both ends of MWD in the case of the sample of high DAM-content (DA3032).

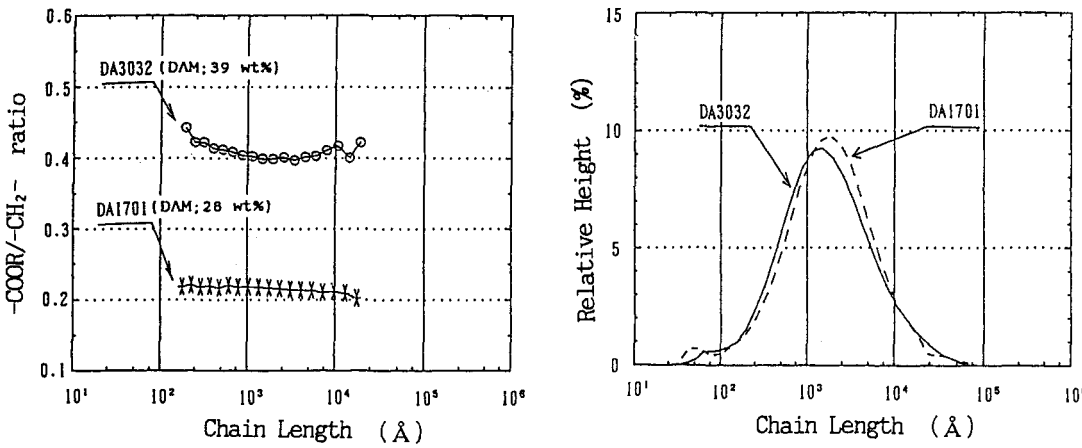

Fig. 12. Molecular weight dependence of DAM-content (left) and molecular weight distribution (right) for EDAM copolymers measured by GPC-FT/IR. (Chloroform solution, 40°C)

Micro-structure of polymer chain

Figure 13 shows the ^{13}C-NMR spectrum of the representative EDAM copolymer sample, DA1701. In order to assign the peaks precisely, DEPT spectrum and ^{13}C-^{1}H correlation 2D spectrum were measured. The former technique is useful to distinguish the number of protons attached to carbon. In this pulse technique, quaternary carbons do not appear, and only CH carbons appear in the case of 90° ^{1}H pulse. All the CH_3, CH_2 and CH peaks appear positively by 45° pulse. By 135° pulse, however, CH_2 peaks appear negatively, as opposed to CH_3 and CH ones. Figure 14 shows a normal ^{13}C-NMR spectrum (a) and DEPT spectra ((b) and (c)) of DA1701. The peaks at 46.03 and 45.30 ppm in the spectrum (a) disappeared in DEPT spectra, suggesting that these peaks are due to quaternary carbon. Comparing two DEPT spectra, the peak at 43.39 ppm can be assigned to CH_2 carbon.

^{13}C-^{1}H correlation 2D spectrum makes ^{13}C-NMR peak assignment easier by using cross peaks linked with ^{1}H-NMR peaks as shown in Fig. 15.

Besides the peaks due to DAM comonomer sequences, many other peaks derived from alkyl short chain branching are observed in ^{13}C-NMR spectrum. Assignments for these peaks were carried out by using Lindeman-Adams empirical equation (ref. 11) and by refering to the reported assignments for high-pressure low density polyethylene (ref. 12-16) and shown in Table 4. It is interesting that both kinds of EDAM samples do not have any peaks due to ethyl branching but have peaks due to n-butyl branching and branchings equal to and longer than n-hexyl. The EDAM copolymer containing more DAM comonomer has less alkyl branchings as shown in the same table. It is

TABLE 4. Degree of alkyl branching in EDAM copolymer.

Sample	DAM	M I	n-Butyl [a)]	≧ n-Hexyl [b)]
	wt%	g/10min.	1/1000C	1/1000C
DA1701	28	100	4.02(4.27) [c)]	5.33(5.67) [c)]
DA3032	39	300	1.75(1.96) [c)]	2.06(2.31) [c)]

a)Ethyl branching was not observed in both samples.
b)Including long chain branching.
c)Calculated on the basis of only ethylene carbons.

suggested by those results that the 1st back-biting reaction which results in alkyl branchings (ref. 17-19), not to speak of the 2nd one, becomes more difficult to occur toward growing radical species with increasing bulky DAM sequences.

In the most up-field region, i.e., in alkyl CH_3 region, the small peaks was observed at 8.87 ppm. This peak can be considered to be due to the end alkyl CH_3 because it increases with decreasing molecular weight. Since some kinds of end structure are probable, chemical shift of CH_3 carbon for each structure was calculated using Lindeman-Adams equation (ref. 11). As a result, the structure shown in Fig. 13 was estimated to be the most plausible one (calculated chemical shift is 8.86 ppm).

In Table 5, the whole assignments for chemical shifts in ^{13}C-NMR spectra of EDAM copolymers are summarized, and the chemical structures corresponding to each assignment are shown in Fig. 16.

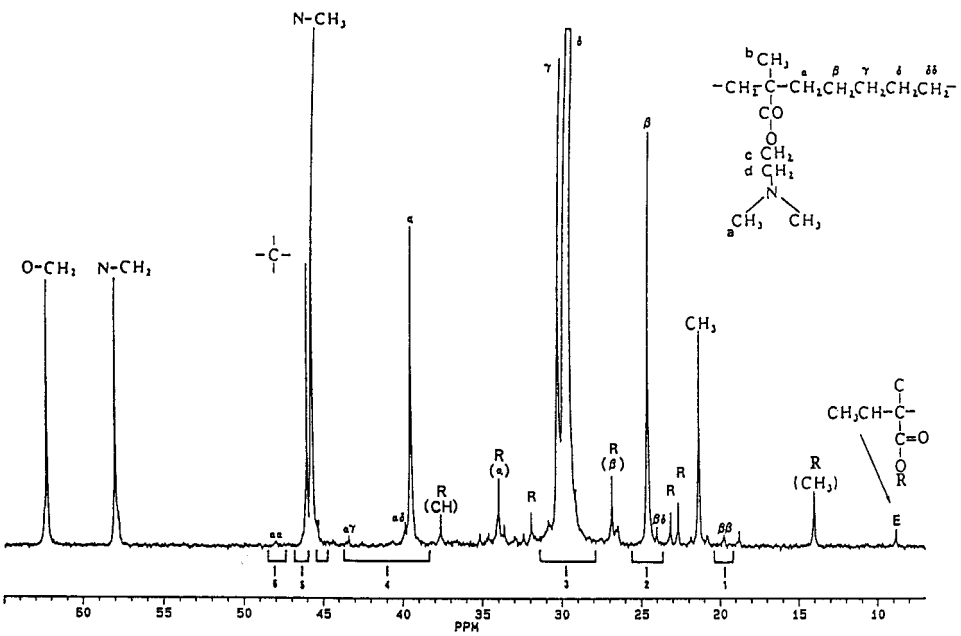

Fig. 13. ^{13}C-NMR spectrum of DA1701 without 3-coupling and NOE. ($CDCl_3$ solution, 60 °C, 100MHz)

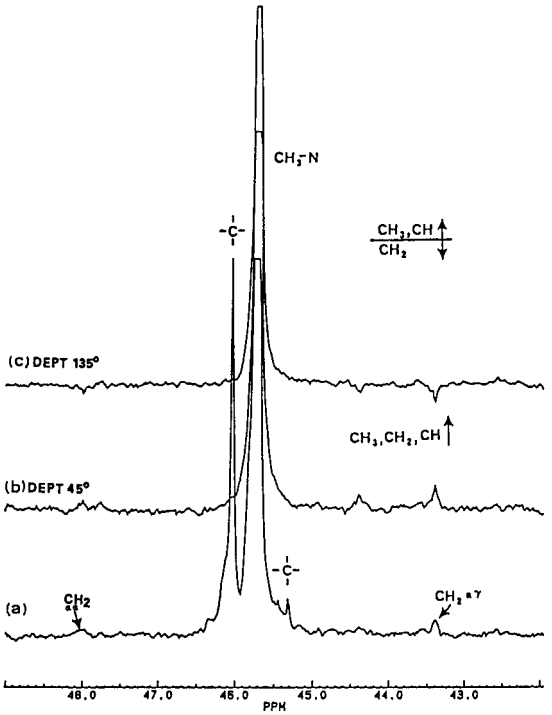

Fig. 14. Alkane region of ^{13}C-NMR spectrum of DA1701 (a), and DEPT spectra measured with 45° (b) and 135 ° (c) pulses. In the spectrum (b), methyl, methylene and methylidyne groups appear positively, whereas methylene group negatively.

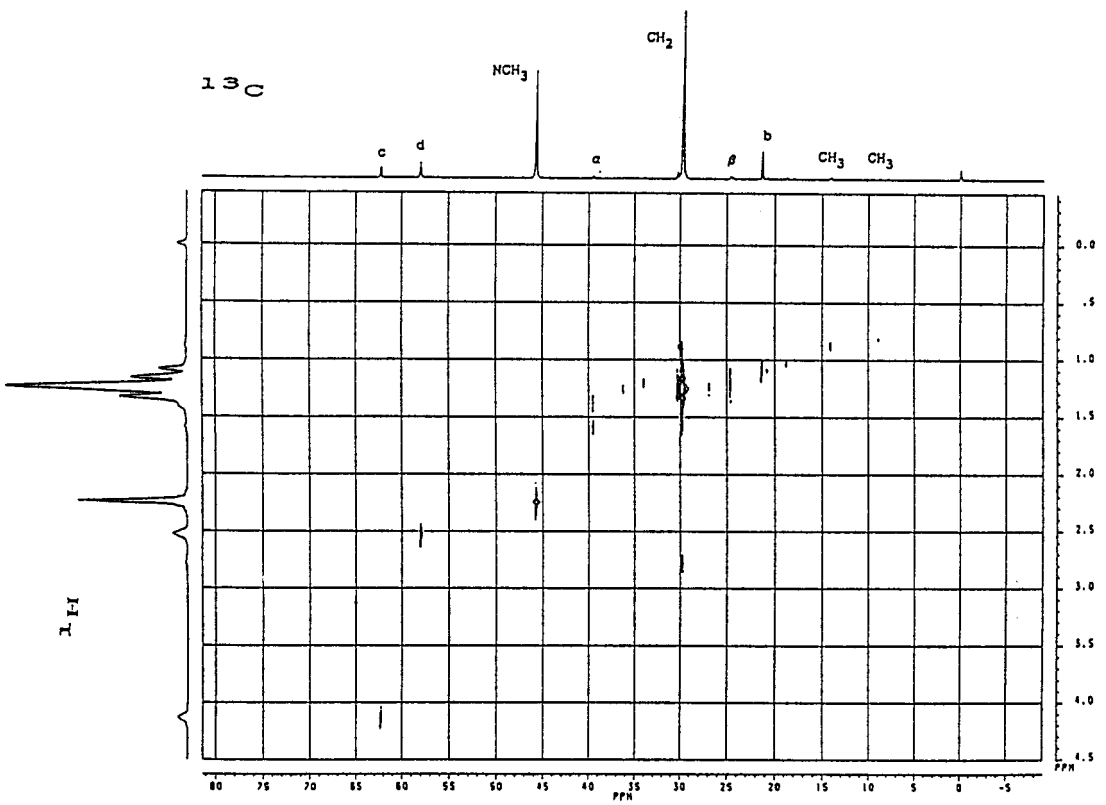

Fig. 15. ^{1}H-^{13}C correlation 2D NMR spectrum of DA1701.

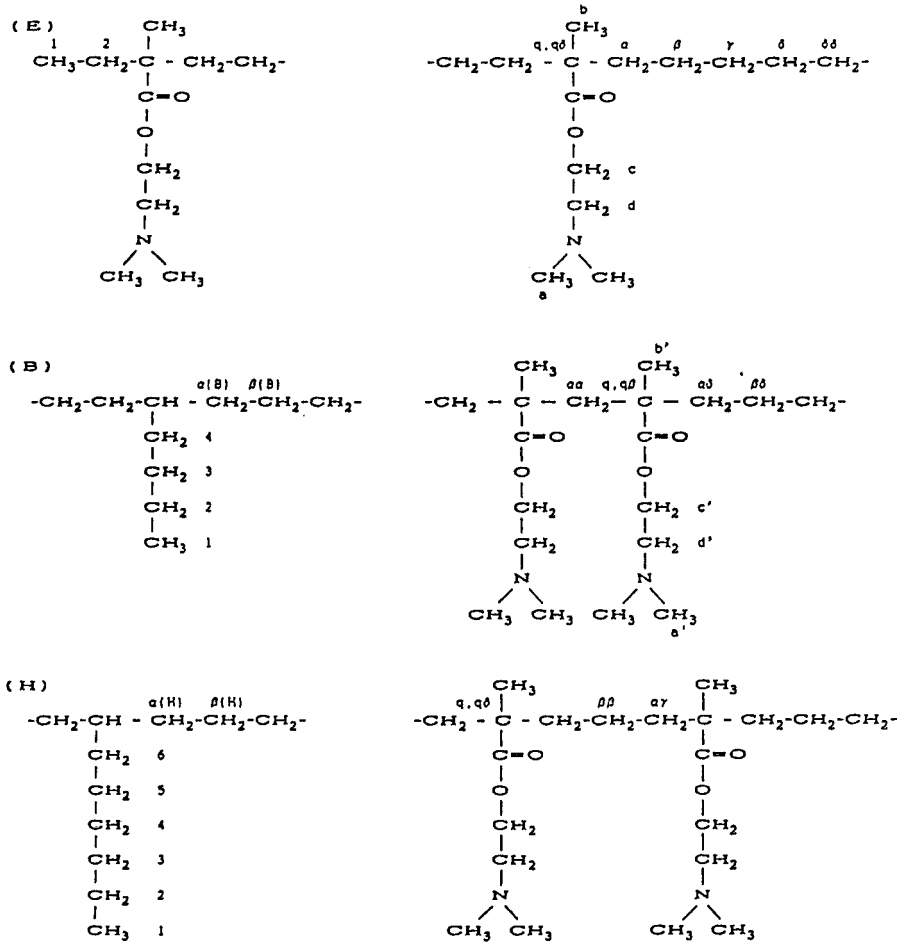

Fig. 16. Structures of chemical shift assignment in ^{13}C-NMR spectra of EDAM copolymer.

Comonomer sequence distribution

The monomer composition, and diad triad sequence distributions of EDAM copolymers can be calculated from ^{13}C-NMR peak intensities of alkane region by the following eqs. (8)~(23), where E and M indicate ethylene and DAM, respectively, and I_n denotes the peak intensity in each region defined in Fig. 13 and Table 5.

$$[MM] = \alpha\,\alpha \tag{8}$$
$$[EM] = \alpha\,\gamma + \alpha + \alpha\,\delta \tag{9}$$
$$[EE] = (\delta\,\delta + \delta + \beta + \beta\,\delta)/2 + \gamma/4 \tag{10}$$

$$[MMM] = 0.0 \tag{11}$$
$$[MME] = 2 \times I_6 \tag{12}$$
$$[MEM] = I_1 \tag{13}$$
$$[EME] = I_5 \tag{14}$$
$$[EEM] = (I_2 + I_4 - 2 \times [MEM])/2 \tag{15}$$
$$[EEE] = (I_3 - [MEE]/2)/2 \tag{16}$$

$$I_{total} = [EEE] + [EEM] + [EME] + [MEM] + [MME] + [MMM] \tag{17}$$
$$EEE = [EEE]/I_{total}, \text{ and so on.}$$

TABLE 5. Chemical shift assignment in ^{13}C-NMR spectra of EDAM copolymers.

Chemical shift	Relative intensity Sample A DA1701 [DAM 28wt%]	Relative intensity Sample B DA3032 [DAM 39wt%]	Intensity ratio B/A	Assignment
8.86	3.0	6.9	2.30	CH_3(E)1
14.09	11.9	10.4	0.87	CH_3(B)1,CH_3(H)1
18.76	2.8	13.3	4.75	b'
19.70	3.2	9.8	3.06	$\beta\beta$
21.32	37.9	92.9	2.45	b
21.85	2.0	6.7	3.35	
22.68	7.7	4.0	0.52	CH_2(H)2
23.17	5.8	3.4	0.59	CH_2(B)2
24.05	3.5	16.6	4.74	$\beta\delta$
24.61	73.0	155.1	2.12	β
26.68	12.6	7.1	0.56	β(B),β(H),CH_2(H)5
29.57	119.6	236.6	1.98	δ
29.72	1000.0	1000.0	1.00	$\delta\delta$, CH_2(B)3
30.27	92.7	187.1	2.02	γ, γ(B), γ(H)
30.88	10.3	19.7	1.91	CH_2(E)2
31.97	6.6	-	-	CH_2(H)3
34.01	16.0	12.1	0.76	α(B),α(H),CH_2(H)6
37.65	7.4	5.8	0.78	CH(B),CH(H)
39.50	71.2	156.1	2.19	α
39.86	5.9	26.1	4.42	$\alpha\delta$
40.70	1.6	5.1	3.19	(qβ)
43.39	3.2	10.1	3.16	$\alpha\gamma$
45.30	4.1	21.5	5.24	qδ
45.71	105.6	270.7	2.56	a,a'
46.03	36.7	95.1	2.59	q
48.10	1.7	5.0	2.94	$\alpha\alpha$
57.75	6.1	30.4	4.98	d'
57.97	40.1	91.1	2.27	d
62.31	41.5	94.8	2.28	c
62.51	5.7	26.4	4.63	c'

(E):End structure
(B):Sequence containing n-butyl branching
(H):Sequence containing n-hexyl branching

TABLE 6. Monomer composition, and diad and triad sequence distributions of EDAM copolymers.

	DA1701 [DAM 28wt%]	DA3032 [DAM 39wt%]
E	93.89	89.33
M	6.11	10.67
EE	88.34	79.19
EM	11.42	20.28
MM	0.24	0.53
EEE	82.93	68.78
EEM	10.62	17.71
EME	5.76	11.99
MEM	0.45	1.01
MME	0.24	0.51
MMM	0.00	0.00

E:Ethylene, M:DAM

TABLE 7. Run numbers (R), numerical average sequence lengths ($\overline{\ell}$), relative monomer reactivity ratios($r_1 \cdot r_2$), and persistence ratios (ρ) calculated from ^{13}C-NMR data.

	DA1701	DA3032
R	11.42	20.28
R_{random}	11.47	19.06
$\overline{\ell}_E$	16.4	8.81
$\overline{\ell}_{E,random}$	16.4	9.37
$\overline{\ell}_M$	1.07	1.05
$\overline{\ell}_{M,random}$	1.06	1.12
$r_1 \cdot r_2$	0.65	0.41
ρ	1.0	0.94

E:Ethylene, M:DAM

$\rho>1$, $r_1 \cdot r_2>1$; block character
$\rho=1$, $r_1 \cdot r_2=1$; random (Bernoullian)
$\rho<1$, $r_1 \cdot r_2<1$; alternate tendency

Peak intensity of each region;

$$I_1 = \beta\,\beta \quad (18)$$
$$I_2 = \beta + \beta\,\delta \quad (19)$$
$$I_3 = \delta\,\delta + \delta + \gamma \quad (20)$$
$$I_4 = \alpha + \alpha\,\delta + \alpha\,\gamma \quad (21)$$
$$I_5 = q\,\beta + q \quad (22)$$
$$I_6 = \alpha\,\alpha \quad (23)$$

The calculated results are listed in Table 6. It is interesting that isolated M units are predominant in the chain microstructure and alternating MEM sequences appear much more than block-like MME sequences.

In order to discuss the randomness of the sequence more quantitatively, some statistical treatments were applied and results are described in Table 7. The product of monomer reactivity ratio ($r_1 \cdot r_2$) is less than 1.0, suggesting the copolymerization mode to be alternating.

Comonomer sequence distribution simulated with the probability theory

For the purpose of confirming both the pertinency of the comonomer sequence distribution and the alternating copolymerization tendency as estimated by the above ^{13}C-NMR investigations, some simulation studies were carried out by applying the probability theory (ref.20) with the assumption of complete mixing continuous flow model and statistical stationarity.

Firstly, Q-e values for E (M_1) and DAM (M_2) were adopted as shown in Table 8 by making reference to the prior studies (ref. 21-22), regardless of different counter comonomers and copolymerization conditions.
Secondly, r_1 and r_2 values (comonomer reactivity ratio) were calculated to be 0.03 and 14.7, respectively, according to Alfrey-Price equation (ref. 23). The product (0.44) of these r_1 and r_2 is not very different from that (0.53) by ^{13}C-NMR estimation.

Thirdly, the copolymer composition, diad concentration and triad fraction were calculated with the r_1 and r_2 values by using Mayo-Lewis equation (ref. 24), Ito's procedure (ref. 20) and the actual data of ethylene conversion in each polymerization (10% for DA1701 and 9% for DA3032). In course of this calculation, the Terminal Model (ref. 20), a stationary Markov process of first order (ref. 25) in which the last one monomer unit in the growing polymer chain affect the probability of monomer addition, was assumed after checking its applicability with ^{13}C-NMR data shown in Table 6. Lastly, run numbers (R), numerical average sequence length ($\bar{\ell}$), and persistence ratio (ρ) were calculated with the general statistical process developed by Coleman and Fox (ref. 26).

All the results calculated according to the above procedures are listed in Table 9 together with those by ^{13}C-NMR estimation. It is surprising that good coincidence is recognized as a whole between two different ways of estimation. This may be resulted from the propriety of the treatment of each ^{13}C-NMR peak on one hand and Q-e values adopted from the literatures on the other, regardless of high-pressure and high-temperature polymerization conditions.

As for the alternating copolymerization tendency, a small ambiguity for random manner (Bernoullian) still remains, because the persistence ratio (ρ) is close to 1.0 in cases of DA1701 and DA3032, in

which DAM-contents are not large enough to distinguish. The additional simulation done on the supposition of a copolymer of 85 wt% (nearly 50 mol%) DAM-content, however, clearly leads to the alternating copolymerization tendency as shown in Table 10 (ρ=0.83).

As a conclusion, the real mode of copolymerization between E and DAM is alternating, although it looks quite close to random copolymerization under lower DAM-content condition.

Crystallinity and lamellar thickness

X-ray crystallinity X_c and unit cell dimension (a,b) of EDAM copolymers having various DAM-content were measured by WAXD analysis, and are shown in Figs. 17, 18, and 19, and in Table 11.

Crystallinity X_c clearly decreases with increasing DAM-content, while a-lattice dimension increases. The increase of b-lattice dimension with DAM-content, however, is not so much as that of a-lattice one. Comparing the results on the same DAM-content (4.3 mol%, for example), the EDAM copolymer of lower molecular weight, namely higher MI, has lower crystallinity X_c.

Lamellar thickness ℓ_c which was determined from long period L by SAXS and crystallinity X_c using eq. (1), decreases with increasing DAM-content as shown in Fig. 20.

The changes in X_c lattice dimensions, and ℓ_c with comonomer content have been reported for ethylene/α-olefin copolymers (ref. 27--32) for many years, and the location of short chain branching in a solid polyethylene has been a subject of controversy for a long time. X-ray diffraction (XRD) has been used most frequently for the analysis of the crystalline region has been discussed on the basis of crystal lattice expansion with increase in the content of branches. Assuming that accommodation of branches within the crystal lattice results in "a 2gl kink defect" (ref. 33), it is suggested that the amount of branches in the crystalline phase can be estimated (ref. 30). However, as several authors have indicated (ref. 34-37), the lamellar crystal thickness itself largely affects the unit cell dimension; the thinner the lamellae, the more the unit cell is expanded. Therefore, it seems reasonable to consider that the XRD method does not necessarily evaluate only the branches included in the crystal but rather the overall effect of the branches on crystalline morphology.

TABLE 8. Q-e values adopted for simulation of comonomer sequence distribution.

Comonomer	Q	e	Counter monomer [a)] and copolymerization condition [b)]
Ethylene (ref. 21)	0.03	-0.43	n-Butyl-acrylate, vinyl-chloride, vinyl acetate, 1000 atm, 70～90℃, toluene solution
DAM (ref. 22)	0.68	0.48	Styrene, 60℃ (no further description)

a),b): descriptions in the cited references (ref. 21-22)

TABLE 9. Comparison of comonomer sequence distribution in EDAM copolymers obtained from ^{13}C-NMR data with that from simulation.

Sample name	DA1701		DA3032	
Test method	^{13}C-NMR data	Simulation	^{13}C-NMR data	Simulation
Feed concentration of DAM (wt%)	–	4.39	–	7.31
Conversion of ethylene (%)	10	10	9	9
(1) Composition [a)]				
P_1 {E}	93.89	94.0	89.33	89.4
P_1 {M}	6.11 (26.7 wt%)	6.03 (26.4 wt%)	10.67 (40.1 wt%)	10.6 (39.8 wt%)
(2) Diad [a)]				
P_2 {EE}	88.34	88.1	79.19	79.4
P_2 {EM} + P_2 {EM}	11.42	11.7	20.28	20.0
P_2 {MM}	0.24	0.17	0.53	0.56
(3) Triad [a)]				
P_3 {EEE}	82.93	82.6	68.78	70.5
P_3 {EEM} + P_3 {MEE}	10.62	11.0	17.71	17.8
P_3 {EME}	5.76	5.69	11.99	9.50
P_3 {MEM}	0.45	0.36	1.01	1.12
P_3 {MME} + P_3 {EMM}	0.24	0.33	0.51	1.06
P_3 {MMM}	0.00	0.00	0.00	0.03
(4) Run number, etc.				
R (Run number)	11.42	11.7	20.28	20.1
R_{random}	11.47	11.3	19.06	18.9
ℓ_E	16.4	16.1	8.81	8.92
$\ell_{E,random}$	16.4	16.6	9.37	9.45
ℓ_M	1.07	1.03	1.05	1.06
$\ell_{M,random}$	1.06	1.06	1.12	1.12
ρ (Persistence ratio)	1.00	0.97	0.94	0.94
$r_1 \times r_2$ product	0.65	0.441	0.41	0.441

a) E:Ethylene, M:DAM

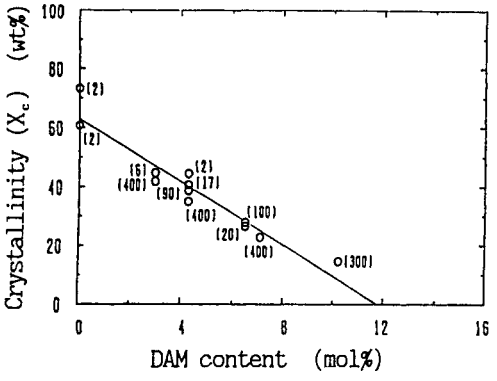

Fig. 17. X-ray crystallinity vs. DAM-content correlation for EDAM copolymers. Numerals in branckets show melt flow index (MI).

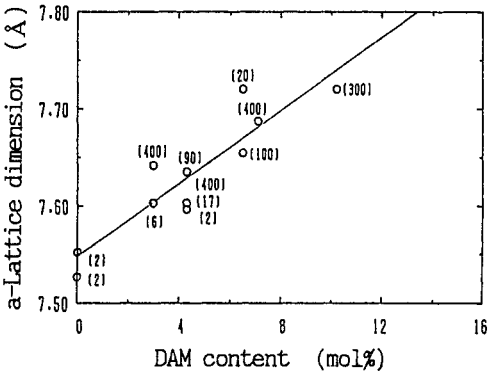

Fig. 18. a-Lattice dimension vs. DAM-content correlation for EDAM copolymers. Numerals in branckets show melt flow index (MI).

TABLE 10. Simulation of comonomer sequence distribution in an EDAM copolymer of 85 wt% DAM content.

Target of DAM content (wt%)	85				
Conversion of ethylene (%)	2	4	6	8	10
Feed concentration of DAM (wt%)	27.8	32.1	36.8	40.9	44.4
DAM content (wt%)	85.6	85.0	85.0	85.0	85.0
(mol%)	51.5	50.3	50.4	50.4	50.3
(1) Composition [a)]					
P_1 {E}	48.5	49.7	49.7	49.6	49.7
P_1 {M}	51.5	50.3	50.4	50.4	50.3
(2) Diad [a)]					
P_2 {EE}	18.5	18.5	19.7	19.6	19.6
P_2 {EM} + P_2 {EM}	60.0	60.1	60.1	60.1	60.1
P_2 {MM}	21.4	20.3	20.3	20.4	20.3
(3) Triad [a)]					
P_3 {EEE}	7.07	7.77	7.74	7.71	7.75
P_3 {EEM} + P_3 {MEE}	22.9	23.8	23.7	23.7	23.7
P_3 {EME}	17.5	18.0	17.9	17.9	17.9
P_3 {MEM}	18.6	18.2	18.2	18.2	18.2
P_3 {MME} + P_3 {EMM}	25.0	24.2	24.2	24.3	24.2
P_3 {MMM}	8.94	8.16	8.19	8.22	8.18
(4) Run number, etc.					
R (Run number)	60.0	60.1	60.1	60.1	60.1
R_{random}	50.0	50.0	50.0	50.0	50.0
ℓ_E	1.62	1.65	1.65	1.65	1.65
$\ell_{E,random}$	1.94	1.99	1.99	1.99	1.99
ℓ_M	1.71	1.67	1.68	1.68	1.68
$\ell_{M,random}$	2.06	2.01	2.01	2.02	2.01
ρ (Persistence ratio)	0.83	0.83	0.83	0.83	0.83
$r_1 \times r_2$ product	0.44	0.44	0.44	0.44	0.44

a) E:Ethylene, M:DAM

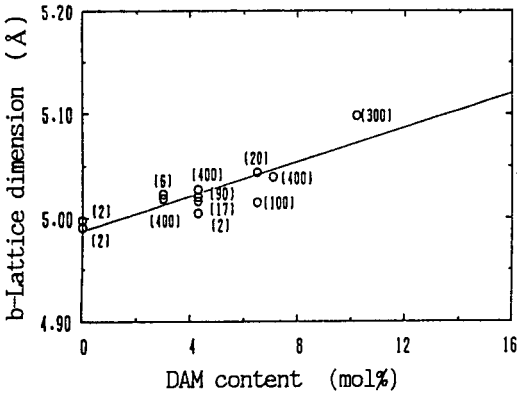

Fig. 19. b-Lattice dimension vs. DAM-content correlation for EDAM copolymers. Numerals in branckets show melt flow index (MI).

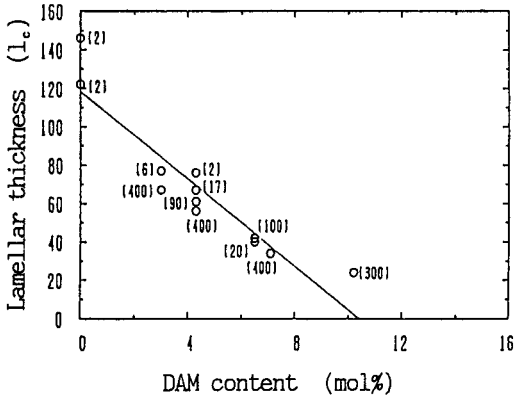

Fig. 20. Lamellar thickness vs. DAM-content correlation for EDAM copolymers. Numerals in branckets show melt flow index (MI).

Recent advanced technique in solid-state NMR revealed that the short chain branchings are located mostly in the amorphous region and partially near the surface of crystalline core (ref. 38-43). Furthermore, the detailed studies on ^{13}C-NMR spectra of the residures from fuming nitric-acid degradation of various ethylene/α-olefin copolymers made it clear that only a small fraction (4～10 %) of total short chain branchings is included in the crystalline region (ref. 44).

Taking these results into consideration, a bulky DAM unit can hardly be included into the crystalline region of EDAM copolymer. Consequently, the lattice expansion with increasing DAM-content described above is considered to be due to the stress on the crystal surface or in the interface region between the amorphous phase and the crystalline core, which is derived from the exclusion of DAM unit to the amorphous region, leading to more surface crowding (ref. 32).

TABLE 11. WAXD and SAXS data of EDAM copolymers.

EDAM	DAM content		M I	L	X_c	ℓ_c	a-Lattice	b-Lattice
	(wt%)	(mol%)	(g/10min.)	(Å)	(wt%)	(Å)	(Å)	(Å)
DA 3032	39	10.2	300	191	14.5	24	7.720	5.098
DA 3002	30	7.1	400	170	22.7	34	7.687	5.039
DA 1701	28	6.5	100	172	27.8	42	7.655	5.015
DA 3012	28	6.5	20	172	26.4	40	7.720	5.043
DA 3023	20	4.3	400	178	34.9	56	7.635	5.027
DA 3011	20	4.3	90	176	38.6	61	7.635	5.020
DA 3013	20	4.3	17	182	40.5	67	7.603	5.016
DA 3014	20	4.3	2	189	44.3	76	7.597	5.004
DA 3024	15	3.0	400	178	41.7	67	7.642	5.018
DA 3005	15	3.0	6	189	44.6	77	7.603	5.023
PE 3341	–	–	2	209	73.3	146	7.552	4.991
PE 3246	–	–	2	215	60.7	122	7.527	4.998

L :Long period determined by SAXS
X_c :Crystallinity
ℓ_c :Lamellar thickness

Spherulites and lamellae morphology

The spherulitic morphology of EDAM copolymer was studied with light scattering photometry. Even small spherulites could be evaluated. As is evident from Figs. 21 and 22, the average size of the spherulite is greatly affected by molecular weight, namely MI, and composition. There is a marked tendency that the diameter of spherulite increases with MI for constant composition, but decreases with DAM-content.

The observation of lamellar crystalline was tried for DA1701 and DA3005 by transmission electron microscopy (TEM). As shown in Fig. 23, thin and waved lamellae were observed, which are similar to those of LDPE prepared by a high-pressure radical polymerization process (ref. 45). The average values of the lamellar thickness obtained from TEM-Image analyzer were approximately 50 Å for both samples, as shown in Table 12, and not affected by DAM-content so much as those by WAXD and SAXS analysis shown in Table 11. The discrepancy between them might come from the ambiguity of this staining and TEM observation method, particularly in lamellae of less than 40 Å thickness. It is supposed that only the amorphous phase is dyed as a result of a relatively easier penetration of the staining reagents, so a clear contrast is visible only when the lamellae and

the amorphous phase are perpendicular to the surface of the thin section. As a matter of fact, the interface contrast in the TEM photograph is fairly obscure as a whole compared to that of HDPE or LDPE (ref. 45), which might lead to the lack of reliability.

As for the lamellae morphology, slit-desmeared SAXS studies were also carried out separately in Chungchun Institute of Applied Chemistry, Chinese Academy of Sciences, and it was considered from the results of Buchanan's procedure (ref. 46) on the SAXS curves that the long period, lamellar thickness, and one-dimensional crystallinity of EDAM copolymers are hardly changed with DAM-content. This

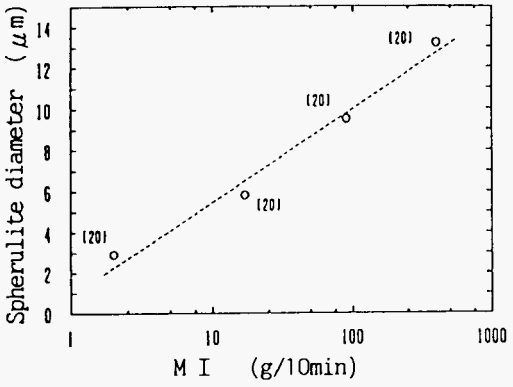

Fig. 21. Spherulite diameter in average vs. MI correlation for EDAM copolymers. Numerals in branckets show DAM-content (wt%).

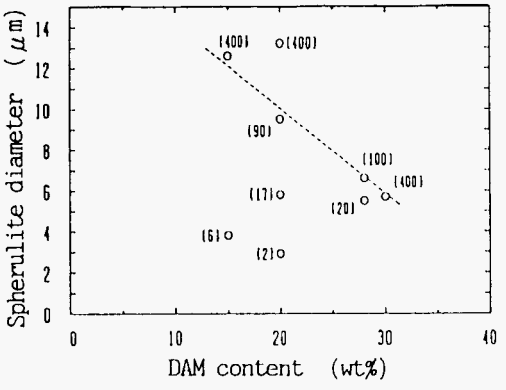

Fig. 22. Spherulite diameter in average vs. DAM-content correlation for EDAM copolymers.
Numerals in branckets show melt flow index (MI).

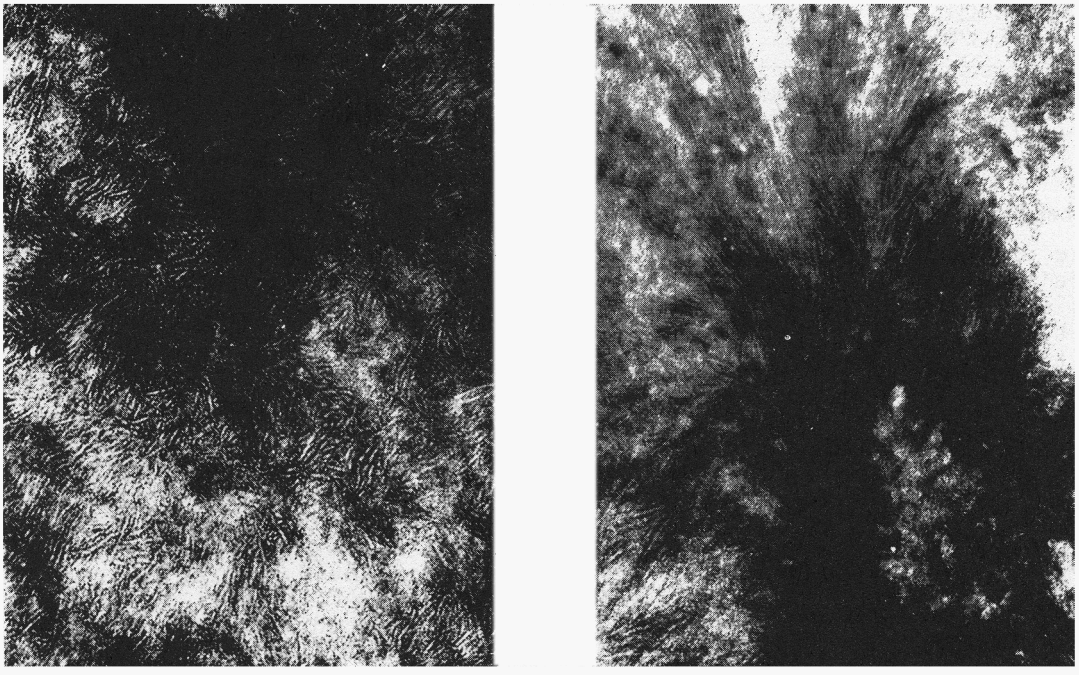

Fig. 23. TEM photographs of lamellae in EDAM copolymers. (Magnification:60,000)

TABLE 12. Lamellar thickness observed by TEM-Image analyzer.

Sample	M I (g/10min.)	DAM content (wt%)	Number of lamellae counted a)	Number average thickness of lamellae (Å)	Lamellae thickness by WAXD and SAXS analysis (Å)
DA3005	6	15	173	54	77
DA1701	100	28	165	51	42

a)Area observed: 2.82×105 nm², Magnification: 60,000

suggestion, however, is quite inconsistent with the correlation of DAM-content to melting point T_m and heat of fusion $\triangle H_f$ which will be discussed in the next section, and consequently remains as a subject to be studied further.

Correlation of crystalline and thermal characteristics

It is very interesting to note that quite good pairwise linear correlations are obtained among crystallinity (X_c by WAXD), lamellar thickness (ℓ_c by WAXD and SAXS) and heat of fusion ($\triangle H_f$ by DSC), by plotting all the related experimental values for EDAM copolymers and LDPEs listed in Table 1 and Table 11, as shown in Figs. 24 and 25.

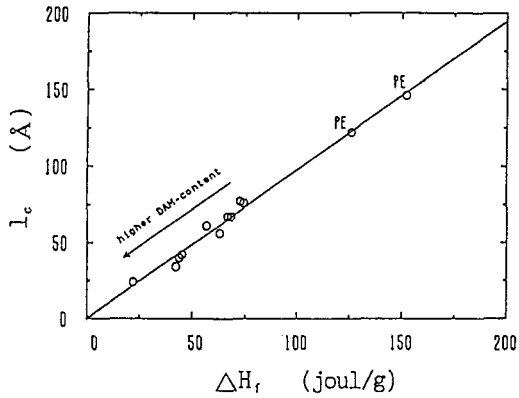

Fig. 24. Lamellar thickness (l_c) vs. heat of fusion ($\triangle H_f$) correlation for EDAM copolymers.
Lamellar thickness:estimated by WAXD and SAXS.
Heat of fusion:estimated by DSC.

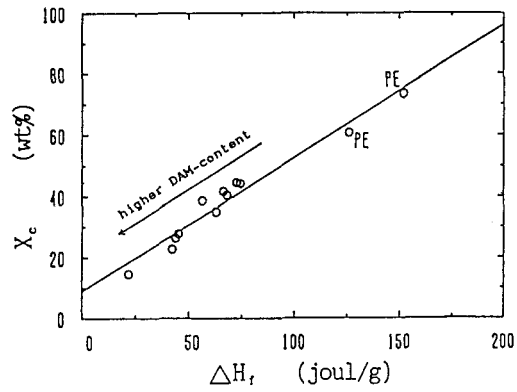

Fig. 25. Crystallinity (X_c) vs. heat of fusion ($\triangle H_f$) correlation for EDAM copolymers.
Crystallinity:estimated by WAXD.
Heat of fusion:estimated by DSC.

As is known as the Thomson-Gibbs equation, lamellar thickness can also be correlated to melting point (ref. 44,47),

$$T_m = T_m^\circ [1 - (2\sigma_e / \triangle h_f \cdot \ell_c)] \qquad (24)$$

where T_m is the observed melting point, T_m° is the equilibrium melting point of an infinite polyethylene crystal, $\triangle h_f$ is the enthalpy of fusion per unit volume, σ_e is the surface free energy of polyethylene crystal, and ℓ_c is the thickness of lamellae with melting point T_m. Lamellar thickness ℓ_c for each EDAM copolymer

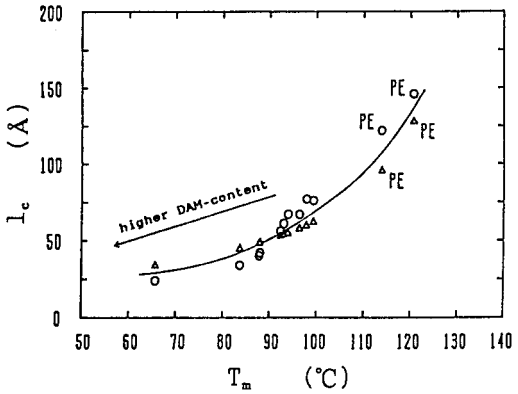

Fig. 26. Lamellar thickness (l_c) vs. melting point (T_m) correlation for EDAM copolymers.
○ ····· l_c estimated by WAXD and SAXS (eq. 1).
△ ····· l_c estimated by DSC (eq. 24).

and LDPE was calculated with its melting point (T_m by DSC listed in Table 1, though not equilibrium ones), from the eq. (24) by using the numerical values for linear unbranched PE as follows (ref. 48): T_m° =414°K, σ_e =87 mJ/m², Δh_f =2.78 ×10⁸ J/m³. As is evident from Fig. 26, the resulting ℓ_c vs. T_m plot shows a smooth relation.

Lamellar thickness estimated from eq.(1) from WAXD and SAXS measurements was also plotted in Fig. 26. A satisfactory agreement is recognized as a whole between the two independent ways of estimation, which supports the validity of the experimental data observed and procedures adopted as for crystalline and thermal characteristics.

Acknowledgements

The authors would like to express their gratitude to the following researchers for their careful analyses and helpful discussions, and also to Sumitomo Chemical Co., Ltd. for permission to publish this paper.

Sumitomo Chemical Co., Ltd.
Mr. Masashi Sakurai (molecular characteristics)

Institute of Chemistry, Chinese Academy of Sciences, Beijing, China
Dr. Shannong Zhu (NMR)
Ms. Jingshu Shen (morphology)

Changchun Institute of Applied Chemistry, Chinese Academy of Sciences, Changchun, China
Ms. Jinyu Huang (DSC and X-ray analyses)
Ms. Wei Li (DSC and X-ray analyses)

REFERENCES

1. Y. Tatsukami, J. Chem. Soc. Japan, 12, 1696 (1978).
2. I. Taniguchi, K. Maemoto, Y. Tatsukami and Y. Kobayashi, U. S. Patent 3,395,198 (1968).
3. C. F. Hammer, U. S. Patent 3,653,803 (1972).
4. S. Hashizume, S. Abeta, T. Ohmae and H. Nishibara, U. S. Patent 4,411,666 (1983).
5. T. Ohmae, N. Yamaguchi, A. Kondo and T. Okada, U. S. Patent 4,721,761 (1988).
6. W. Dollbopf, H. P. Grossmann and U. Leute, Colloid Polym. Sci., Polym. Phys. Ed., 17, 1211 (1979).
7. R. S. Stein and M. B. Rhodes, J. Appl. Phys., 31, 1873 (1960).
8. I. Harris, J. Polym. Sci., 8, 353 (1952).
9. H. Benoît and D. Froelich, Light Scattering from Polymer Solution, Chapter 11, M. B. Huglin, Ed., Academic Press, New York (1972).

10. L. Bohn, Polymer Handbook, Section III, p. 242, J. Bandrup and E. H. Immergut, Eds., Wiley-Interscience, New York (1975).
11. L. P. Lindeman and J. Q. Adams, Anal. Chem., 43, 1245 (1971).
12. D. E. Dorman, E. P. Otocka and F. A. Bovey, Macromolecules, 5, 574 (1972).
13. J. C. Randall, J. Polym. Sci., Polym. Phys. Ed., 11, 275 (1973).
14. T. Hata, T. Suzuki and K. Kosaka, Kobunshi Ronbunshu, 32, 91 (1975).
15. A. Nishioka, Y. Mukai, S. Ohuchi and T. Imanari, Bunseki Kagaku, 29, 774 (1980).
16. S. Ohuchi, T. Imanari, Y. Mukai and A. Nishioka, Bunseki Kagaku, 30, 332 (1981).
17. S. Kita and K. Fukui, Kobunshi Kagaku, 24, 348 (1967).
18. P. L. Nicolas, J. Chem. Phys., 55, 177 (1958).
19. M. J. Wiscotsky, A. E. Kober and I. A. Zlochower, J. Appl. Polym. Sci., 15, 1737 (1971).
20. K. Ito and Y. Yamashita, J. Polym. Sci., A3, 2165 (1965).
21. R. D. Burkhart and N. L. Zutty, J. Polym. Sci., A1, 1137 (1963).
22. L. J. Young, J. Polym. Sci., 54, 411 (1961).
23. T. Alfrey and C. C. Price, J. Polym. Sci., 2, 101 (1947).
24. F. R. Mayo and F. M. Lewis, J. Am. Chem. Soc., 66, 1594 (1944).
25. F. P. Price, J. Chem. Phys., 36, 209 (1962).
26. B. D. Coleman and T. G. Fox, J. Polym. Sci., A1, 3183 (1963).
27. P. R. Swan, J. Polym. Sci., 56, 409 (1962).
28. C. H. Baker and L. Mandelkern, Polymer, 9, 71 (1966).
29. K. Sirayama, S. Kita and H. Watanabe, Makromol. Chem., 151, 97 (1972).
30. F. J. Balta'Calleja, J. C. Gonza'lez Ortega and J. Martinez Salazar, J. Polymer, 19, 1094 (1978).
31. M. Sa'nchez Cuesta, J. Martinez Salazar and F. J. Balta'Calleja, Polym. Bull., 17, 23 (1987).
32. P. R. Haward and B. Brist, J. Polym. Sci., Polym. Phys. Ed., 27, 2269 (1989).
33. B. Wunderlich, Macromolecular Physics, Vol. 1, p. 446, Academic Press (1973).
34. D. J. Cutler, P. J. Hendra, M. E. A. Cudby and H. A. Willis, Polymer, 18, 1005 (1977).
35. B. G. Landes and I. R. Harrison, Polymer, 28, 911 (1987).
36. G. T. Davis, R. K. Eby and J. P. Colson, J. Appl. Phys., 41, 4316 (1970).
37. R. Kitamura and L. Mandelkern, J. Appl. Polym. Sci., A2, 8, 2079 (1970).
38. D. C. McFaddin, K. E. Rusell and E. C. Kelusky, Polym. Commun., 27, 204 (1986).
39. D. C. McFaddin, K. E. Rusell and E. C. Kelusky, Polym. Commun., 29, 258 (1988).
40. D. L. VanderHart and E. Pe'rez, Macromolecules, 19, 1902 (1986).
41. E. Pe'rez, D. L. VanderHart, B. Crist Jr. and P. R. Howard, Macromolecules, 20, 78 (1987).
42. E. Pe'rez, D. L. VanderHart, J. Polym. Sci., Polym. Phys. Ed., 25, 1637 (1987).
43. F. Laupretre, L. Monnerie, L. Barthelemy, J. P. Varion, A. Sauzeau and D. Roussel, Polym. Bull., 15, 159 (1986).
44. S. Hosoda, H. Nomura, Y. Gotoh and H. Kihara, Polymer, 31, 1999 (1990).
45. S. Hosoda, K. Kojima and M. Furuta, Makromol. Chem., 187, 1501 (1986).
46. D. R. Buchanan, J. Polym. Sci., A2, 9, 645 (1971).
47. B. Wunderlich, Macromolecular Physics, Vol. 3, p. 30, Academic Press (1983).
48. B. Wunderlich, Macromolecular Physics, Vol. 3, p. 32, Academic Press (1983).